



## Charge-transfer dynamics in one-dimensional C<sub>60</sub> chains

V. Pérez-Dieste<sup>a,1</sup>, A. Tamai<sup>b,2</sup>, T. Greber<sup>b</sup>, S.G. Chiuzbaian<sup>a,3</sup>, L. Patthey<sup>a,\*</sup>

<sup>a</sup>Swiss Light Source, Paul Scherrer Institut, CH-5232 Villigen PSI, Switzerland

<sup>b</sup>Physik-Institut der Universität Zürich, Winterthurerstrasse 190, CH-8057 Zürich, Switzerland

### ARTICLE INFO

#### Article history:

Received 15 January 2008

Accepted for publication 18 March 2008

Available online 7 April 2008

#### Keywords:

Autoionization  
Resonant photoemission  
Core-hole clock  
One-dimensional system  
Fullerenes  
Monoatomic chains  
Charge transfer

### ABSTRACT

Charge transfer in highly-ordered C<sub>60</sub> chains grown on a Cu(553) vicinal surface is studied by means of resonant photoemission. Tuning the light polarization, autoionization of the highest occupied molecular orbital (HOMO) was expected to detect anisotropy in this one-dimensional system. For one monolayer C<sub>60</sub> we found no signature of autoionization. This indicates that for an electron which is excited from the C 1s level of C<sub>60</sub> to the lowest unoccupied molecular orbital (LUMO), hybridization leads to delocalization on the femtosecond time-scale and no influence of the light polarization is observed.

© 2008 Elsevier B.V. All rights reserved.

### 1. Introduction

Self-assembly is a promising method for the integration and patterning of molecular electronic devices with complex circuits at the nanoscale [1,2]. Vicinal surfaces, which exhibit a regular distribution of steps and terraces, are natural templates to guide the assembly of molecules into specific arrangements [3–7]. The convenient terrace and step sizes for a given molecule can be selected in the nanometric scale by tuning the miscut angle. As a result of the combined effect of molecule–molecule and molecule–substrate interactions, single molecular chains can be grown along the step edge. This approach has given very good results for the formation of ordered one-dimensional C<sub>60</sub> chains on metal surfaces [8,9].

C<sub>60</sub> molecules attract a lot of interest because of their prospective role in nanoelectronics [11] and because of the rich transport properties in the solid phase, ranging from metallic to Mott–Hubbard insulating and superconducting behavior, when doped with alkali metals [12]. Due to the high electron affinity of the molecule, adsorption on metal surfaces may also produce a partial filling of the C<sub>60</sub> LUMO (lowest unoccupied molecular orbital) through charge transfer from the substrate [13–15]. Very promising was

the observation of an excitation gap persisting up to 260 K for C<sub>60</sub>/Ag(100), although its superconductor origin is not demonstrated [16–18]. The interaction of the C<sub>60</sub> molecule with the substrate is also decisive in determining its orientation and intermolecular distance. Orientational order was a necessary condition to determine the LUMO band structure in a K<sub>3</sub>C<sub>60</sub> layer on Ag(111) [19]. The dispersion of the C<sub>60</sub>-derived states close to the Fermi level was found to be consistent with band structure calculations renormalized due to the coupling with high-energy phonons.

C<sub>60</sub> on Cu(553) is possibly a good system to study correlation effects and electron–lattice interactions in a one-dimensional molecular system. Tamai et al. have shown that on this vicinal surface, the molecules self-assemble into long-ordered single chains [8,10]. Scanning tunneling microscopy (STM) images display alternating bright and dim rows of molecules. Adjoining chains have a different bonding to the ascending step and molecules are adsorbed either with the hexagon or the pentagon ring facing the substrate terraces (Fig. 1). The presence of a regular array of atomic steps in the surface induces a 4% expansion of the molecular layer in the direction perpendicular to the chains, compared to the solid phase. Angle-resolved photoemission (ARPES) data show that this small increase of the C<sub>60</sub>–C<sub>60</sub> distance is sufficient to produce a very anisotropic band structure, indicative of significantly decoupling of the molecular chains. Along the chains, the HOMO (highest occupied molecular orbital) exhibits up to 400 meV electronic dispersion, whereas in the perpendicular direction the bandwidth is lower than 30 meV [10]. Because of charge transfer from the metal substrate, the LUMO is partially occupied and contributes to the density of states near the Fermi level. Its photoemission lineshape

\* Corresponding author.

E-mail address: [luc.patthey@psi.ch](mailto:luc.patthey@psi.ch) (L. Patthey).

<sup>1</sup> Present address: CELLS-ALBA, Edifici Ciències Nord, Universitat Autònoma de Barcelona, 08193 Bellaterra, Barcelona, Spain.

<sup>2</sup> Present address: School of Physics and Astronomy, University of St. Andrews, North Haugh, St. Andrews, KY 16 9SS, United Kingdom.

<sup>3</sup> Present address: UPMC Univ Paris 06, UMR 7614, Laboratoire de Chimie Physique – Matière et Rayonnement, 11 Rue Pierre et Marie Curie, 75231 Paris Cedex 05, France.

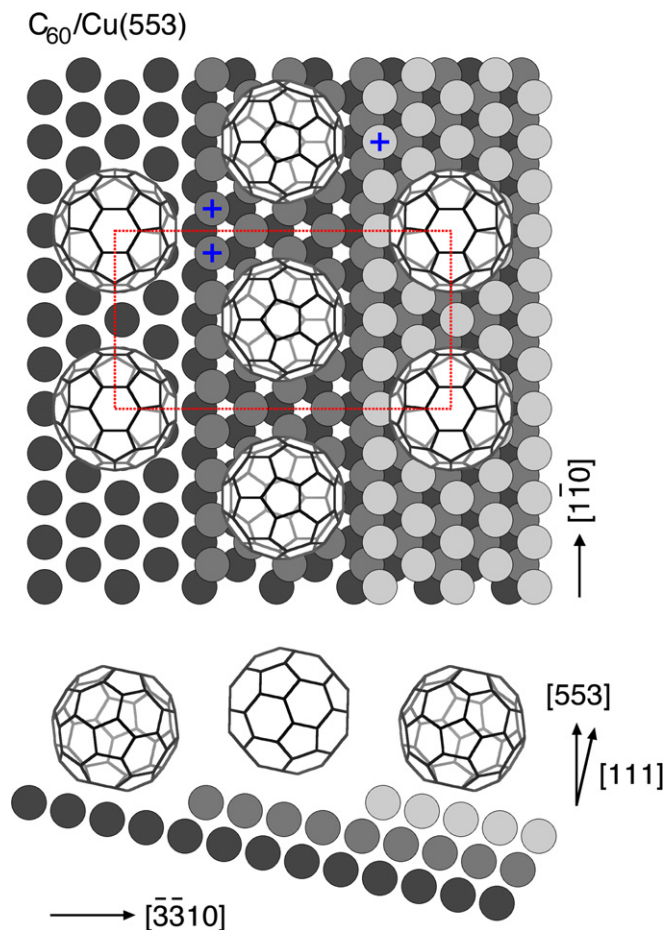


**Fig. 1.** Structural model for C<sub>60</sub> exhibiting alternating chains of hexagon and pentagon bonded molecules, from [10]. The top view is along the [111] direction. The crossed markers show the different coordination to the copper atoms of the step for C<sub>60</sub> of adjoining chains. The side view is along the [110] direction.

is very different from the typical LUMO spectra for two-dimensional C<sub>60</sub> layers: there is a gradual loss of intensity towards the Fermi level and no sharp quasi-particle peak appears. Systematic ARPES measurements display no periodic dispersion near the Fermi level [20].

In order to better understand the molecule–molecule and molecule–substrate electron hopping mechanism, we investigated the C<sub>60</sub> chains by resonant photoemission, also referred to as autoionization [21–23]. From the decay process of an electron excited from a core level to the LUMO it is possible to deduce the electron hopping time-scale for that electron by comparison with the core level lifetime. If the electron is transferred to a neighboring molecule or to the substrate faster than the core level lifetime, the HOMO participant channel is quenched. With this technique, Maxwell et al. proved the hybridization of the core-hole perturbed C<sub>60</sub> orbitals and the sp band of the metal substrate in C<sub>60</sub>/Au(110) [24]. The directional character of the π\* orbitals that form the LUMO in C<sub>60</sub> allows tuning the excitation to different parts of the C<sub>60</sub> molecule by selecting the direction of the light polarization vector, as demonstrated by Maxwell et al. for C<sub>60</sub>/Al(110) [25]. We take advantage of this fact as a complementary method to investigate possible anisotropy in the LUMO derived intermolecular interactions in the directions parallel and perpendicular to the C<sub>60</sub> chains. Our results show that in the case of 0.9 ML C<sub>60</sub>/Cu(553) the anisotropic intermolecular interaction can not be disentangled from the interaction of the molecules with the substrate. No dependence of the substrate–molecule interaction on the light polarization vector is observed.

## 2. Experimental details

The photoemission and absorption measurements were performed at the surface and interface spectroscopy (SIS) beamline at the Swiss Light Source, Paul Scherrer Institut (Villigen, Switzerland). Linear vertical and horizontally polarized light was used. The photoemission spectra were recorded with a Gammadata Scienta 2002 analyzer in angle integration mode. The electron energy resolution in the photoemission data was 140 meV and the photon energy resolution in the absorption data was 100 meV. The photon energy was calibrated using the 3p<sub>3/2</sub> core level measured in the clean Cu substrate and the Cu Fermi level measured at the same photon energy,  $h\nu = 275$  eV. All the data were acquired at room temperature (RT) and the pressure during the measurements remained below  $2 \times 10^{-10}$  mbar.

Cu(553), the stepped surface used in this work, is a B-type vicinal of Cu(111) with a miscut angle of 12.3°. It is composed of (111) terraces separated by monoatomic steps with (11 $\bar{1}$ ) step facets. The nominal terrace width is 9.8 Å, which is close to the van der Waals diameter of the C<sub>60</sub> molecule. The Cu(553) single crystal was cleaned by several cycles of argon ion sputtering at 1000 V and 700 V and annealing at 700 K. C<sub>60</sub> powder (99.9%) was sublimated from a titanium crucible using an evaporation rate of 2 ML/h, as calibrated by XPS. The background pressure during evaporation was kept below  $2 \times 10^{-9}$  mbar. The ordered C<sub>60</sub> chains structure has been obtained by evaporating 1 ML of C<sub>60</sub> onto the surface held at 600 K. The quality of the film was confirmed by the observation of a sharp ( $4 \times 8\frac{2}{3}$ ) LEED pattern [8].

## 3. Results

C 1s core level spectra measured at different C<sub>60</sub> coverage are displayed in Fig. 2. The photon energy was 330 eV, the angle of detection was normal to the surface and the angle of incidence of

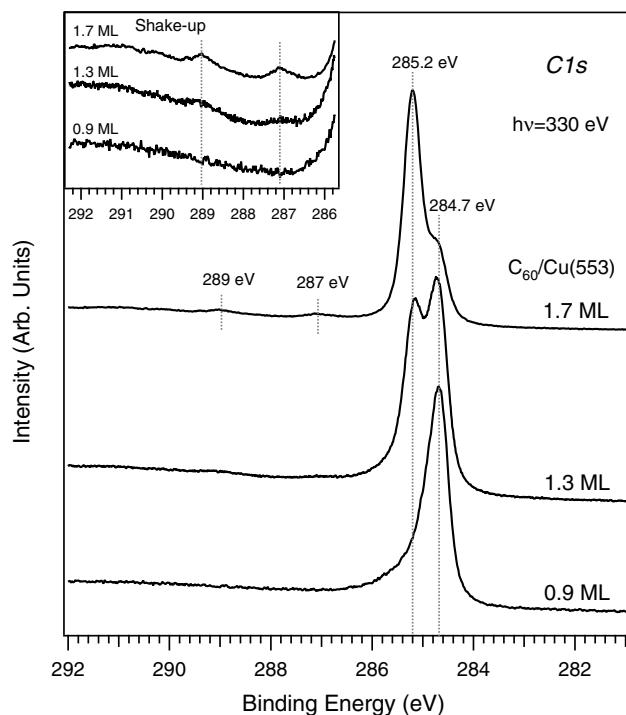


**Fig. 2.** C 1s XPS spectra of C<sub>60</sub>/Cu(553) measured at normal emission with increasing C<sub>60</sub> coverage. The contribution corresponding to molecules in the first layer is shifted towards lower binding energy due to screening from the substrate. A zoom of the satellite region can be seen in the inset at the upper left corner.

the light was  $\theta_{inc} = 45^\circ$ . The spectra are very similar to those obtained for  $C_{60}/Cu(111)$ , described in detail by Tsuei et al. [26]. The coverage of the samples was estimated based on the LEED patterns and on the relative height of the two components in the XPS data for samples with more than 1 ML. The calibration was further confirmed by comparison of our valence band spectra with those from Tsuei et al. [26]. For a coverage over 1 ML there are two components, corresponding to  $C_{60}$  molecules in the second layer and to molecules interacting with the  $Cu(553)$  substrate, which appear at binding energies 285.2 eV and 284.7 eV, respectively. The component due to the first layer is shifted by 0.5 eV towards lower binding energy, indicating screening by the substrate similar to that in  $Cu(110)$  and  $Cu(111)$  [26]. The full width at half maximum (FWHM) is 0.48 eV for the second layer component and 0.64 eV for the first layer component, slightly smaller than the FWHM for the first component on  $Cu(111)$ , 0.73 eV.

For the higher coverage, two satellite peaks are clearly observed at 1.9 eV and 3.7 eV from the peak corresponding to the second  $C_{60}$  layer. For bulk  $C_{60}$ , the shake-up structure contains six features, most of them assigned to transitions between molecular orbitals of the neutral states [26]. The peak that appears at 1.9 eV has been identified as an exciton from HOMO to LUMO derived states. Both satellite features are still visible for 1.3 ML  $C_{60}$  but they are not present in the 0.9 ML film, which is consistent with the fact that chemisorption of the  $C_{60}$  molecules in the first layer involves mixing of the molecular and substrate levels in the initial and final states [27]. For 0.9 ML  $C_{60}$ , the C 1s peak displays an asymmetric line shape. This asymmetry has also been observed in 1 ML  $C_{60}$  on  $Cu(111)$  and on  $Au(110)$  and it has been explained by a distribution of adsorption sites or by the metallic character of the overlayer [24,26]. In our system the different orientations of the  $C_{60}$  molecules in bright and dim chains could also cause a broadening due to the different coordination of the molecules in the two different chains [10].

To precisely determine the resonance photon energy, the C 1s X-ray absorption spectrum was measured. The two curves shown in Fig. 3 correspond to 1.3 ML  $C_{60}$  with the light polarization vector

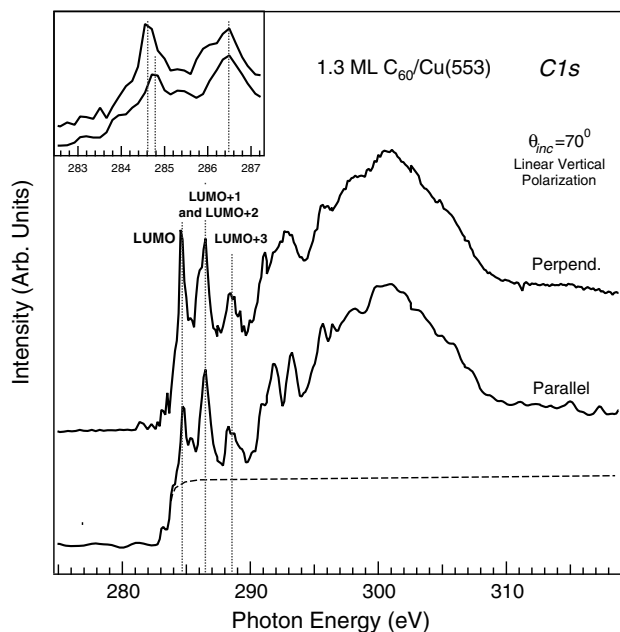


**Fig. 3.** C 1s X-ray absorption spectra for 1.3 ML  $C_{60}/Cu(553)$  with the polarization vector parallel and perpendicular to the  $C_{60}$  chains. The dashed curve indicates the presence of a background step, as expected for a metallic substrate. The inset shows a zoom of the LUMO region, where there is a 0.2 eV shift in the peak position depending on the light vector orientation.

along and perpendicular to the  $C_{60}$  chains. The light was grazing incident and the curves were normalized by the corresponding absorption curve measured in the clean substrate. As can be seen in the inset, the LUMO peak appears at an energy of 284.6 eV in the absorption curve measured with the polarization light vector perpendicular to the  $C_{60}$  chains and at 284.8 eV when it is parallel to the chains. This decrease of energy in the LUMO absorption edge for the perpendicular geometry can be explained by hybridization of the corresponding LUMO orbitals with the steps.

Peaks corresponding to transitions to other  $\pi^*$  levels appear at photon energies 286.5 eV and 288.45 eV. LUMO + 1 and LUMO + 2 levels merge due to the interaction of the  $C_{60}$  molecules with the substrate [26].

The features observed at 293 eV, 296.6 eV and 300.7 eV are due to transitions to  $\sigma$  states. At  $h\nu = 284.1$  eV a step is clearly seen in the absorption spectra which is due to the onset of excitation from the C 1s level to the states above the Fermi level in the metallic substrate.

On the other hand, the energy of the LUMO peaks is very close to the core-level binding energy measured by XPS, indicating that the final states of the two processes are equivalent. This effect is characteristic of metallic overlayers and it is due to screening electrons filling states at the Fermi level in the XPS process, which produces a final state identical to that of the NEXAFS lowest absorption [28]. In agreement with this, in a thick layer of  $C_{60}/Cu(111)$  the energy of the LUMO excitation is 0.7 eV lower than the binding energy of the C 1s XPS feature [26].

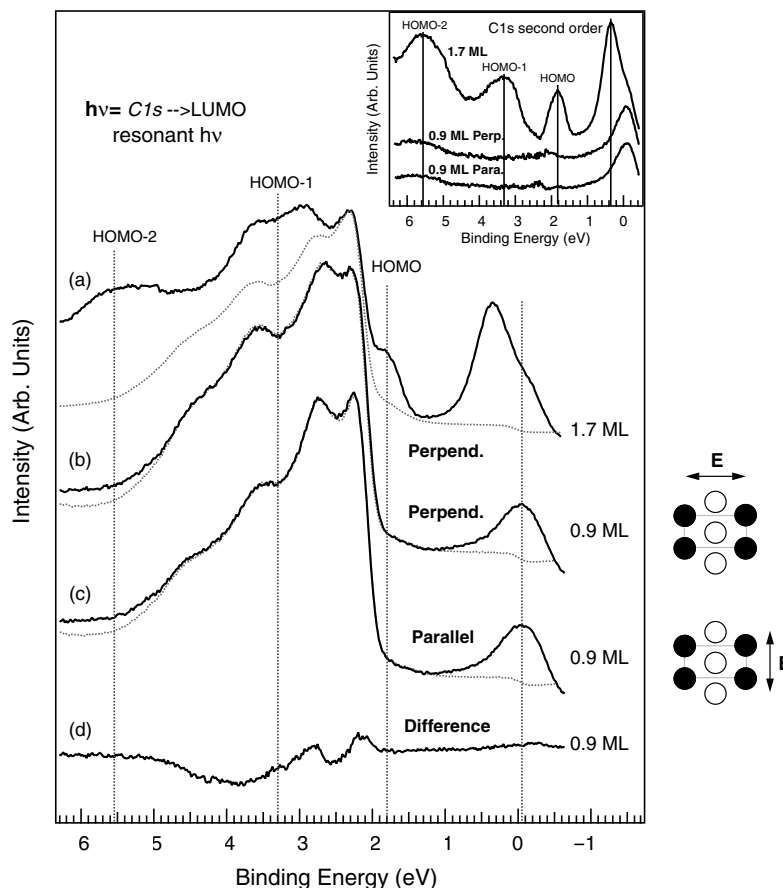
To study the charge transfer dynamics in  $C_{60}$  chains, resonant photoemission measurements were performed with the polarization light vector parallel to the optical surface. The sample was rotated azimuthally in order to place the electric field vector either parallel or perpendicular to the chains.

Fig. 4 shows the valence band photoemission spectra of 0.9 ML  $C_{60}/Cu(553)$  at the resonance energy with the polarization vector perpendicular (curve (b)) and parallel (curve (c)) to the  $C_{60}$  chains. The photon energy was swept across the C 1s LUMO absorption edge in 0.2 eV steps. The expected resonance energy,  $h\nu = 284.7 \pm 0.1$  eV, was determined by the LUMO peak position in the X-ray absorption spectra. As a reference, the resonance spectrum for 1.7 ML  $C_{60}$ , measured with the polarization vector perpendicular to the chains, is shown in curve (a).

Features appearing at 2.3 eV, 2.75 eV and 3.5 eV correspond to the Cu 3d bands. The peak at 0.35 eV in curve (a) and around 0 eV in curves (b) and (c) is due to C 1s 2nd order emission.

For 1.7 ML  $C_{60}$ , clear features corresponding to resonant photoemission from the HOMO, HOMO – 1 and HOMO – 2 levels appear at binding energies 1.76 eV, 3.28 eV and 5.5 eV, respectively, for resonant photon energy  $284.8 \pm 0.25$  eV. In the  $C_{60}$  monolayer spectra (curves (b) and (c)) only the 3d bands from copper are visible when the photon energy is swept across the C 1s absorption edge, between  $h\nu = 283$  eV and  $h\nu = 285.5$  eV. Small variations of those features between curves (a) and (b) are related to anisotropy of those Cu bands. There are no traces of resonance from the HOMO levels in curves (b) and (c). In effect, curve (d) resulting from the subtraction of curves (b) and (c) shows no differences in the HOMO region between the two experimental geometries.

In the inset of Fig. 4, the contribution for photon energies out of resonance has been subtracted from the curves at resonance for 1.7 ML and 0.9 ML  $C_{60}$  with both orientations of the light. It can be seen that for 1.7 ML the HOMO, HOMO – 1 and HOMO – 2 resonant features become clearly visible, while for 0.9 ML those features are not revealed by the subtraction. The photon energy was swept in an interval of 3 eV around the C 1s LUMO absorption edge and no HOMO features were either observed in the resulting subtractions.



**Fig. 4.** C 1s autoionization spectra for  $C_{60}/Cu(553)$  measured at normal incidence with the polarization light vector parallel to the optical surface. (a) 1.7 ML and polarization light vector oriented perpendicular to the  $C_{60}$  chains; (b) and (c) 0.9 ML and polarization light vector oriented perpendicular and parallel to the  $C_{60}$  chains, respectively. The resonance photon energy for 1.7 ML was  $284.8 \pm 0.25$  eV. For 0.9 ML the curves shown correspond to the LUMO peak found in X-ray absorption,  $h\nu = 284.7 \pm 0.1$  eV. (d) Subtraction of curves (b) and (c); there are no visible differences in the HOMO region between excitations with the light vector parallel and perpendicular. In the inset, the autoionization spectra for 1.7 ML and 0.9 ML after out-of-resonance curves subtraction is shown. Those out-of-resonance curves are shown in the main figure in dotted grey.

#### 4. Discussion

Resonant photoemission allows studying charge transfer events in the time-scale of the core-level relaxation time. In this technique, the photon energy is swept through the absorption edge of a given atomic species: here it is the carbon 1s edge. When the photon energy equals the energy difference between the C 1s and LUMO levels, an electron is excited from the C 1s to the LUMO. The relaxation can proceed through several radiative and non-radiative channels. In the so-called autoionization process or participator channel, an electron from the HOMO decays to the C 1s level and the electron from the LUMO is ejected. The final state of this process is the same as the one from the direct photoemission from the HOMO, which simultaneously takes place; an enhancement of the HOMO intensity is expected for the resonant photon energy [21]. The decay is also possible through ejection of an electron from deeper HOMO levels, so-called spectator channels. If the electron excited to the LUMO is transferred to another molecule or to the substrate, faster than the lifetime of the C 1s core-hole, it can not take part in the autoionization process and the decay proceeds through non resonant Auger emission.

To investigate the anisotropy of intermolecular hopping of the LUMO, we have evaluated the dependence of the resonant photoemission features on the direction of the electric field vector. The LUMO orbital of  $C_{60}$  is mainly derived of combinations of  $\pi$  orbitals with radial orientation. Thus, when the polarization vector is parallel to the surface, the C 1s-to-LUMO excitation probability is

enhanced for the orbitals with axes parallel to the surface. When the light vector is perpendicular to the surface, the excitation to orbitals with axes perpendicular to the surface is favored. This has been demonstrated for  $C_{60}/Al(110)$  [25].

Similarly, it should be possible to enhance charge transfer either along or parallel to  $C_{60}$  chains by tuning the light vector in those directions. However, in our experimental data of Fig. 4 it can be seen that for 0.9 ML  $C_{60}/Cu(553)$  no HOMO resonance is observed, indicating a complete delocalization of the excited electron on the LUMO, on the femtosecond time-scale. Only features corresponding to second order C 1s and the Cu d bands are seen in curves (b) and (c), independently of the orientation of the light polarization vector.

The intermolecular hopping for an electron excited to the LUMO in solid  $C_{60}$  has been shown to be negligible due to electron correlations, which localize the excited state to the probed molecule [29]. For  $C_{60}$  chains, the 400 meV dispersion measured for the HOMO by ARPES indicates strong intermolecular coupling along the chains. On the other hand, the  $C_{60}$ - $C_{60}$  distance in the perpendicular direction is 4% larger than along the chains [8] and than in solid  $C_{60}$ . As the hopping between  $C_{60}$   $\pi$  orbitals is very sensitive to the distance between the molecules, the  $C_{60}$  band dispersion is smaller along the perpendicular direction [10].

Therefore, in order to explain the delocalization of the excited electron found in both cases, the  $C_{60}$ -substrate interaction must be taken into account, and it appears to be stronger than the molecule-molecule hybridization. As shown in the previous section,

XPS and NEXAFS data are consistent with a strong  $C_{60}$ -substrate interaction, affecting the electronic structure. In particular it was noticed that very efficient screening from the substrate causes similar final states for the  $C\ 1s \rightarrow$  LUMO NEXAFS and  $C\ 1s$  XPS processes [28]. In those conditions, the autoionization becomes equivalent to Auger decay and the HOMO resonance is not expected anymore. The lack of a visible resonance can be interpreted, similarly to  $C_{60}/Au(110)$ , as the signature of hybridization between the core-hole perturbed  $t_{1u}$  orbital and the  $Cu(553)$  sp band, with bonding interaction larger than the lifetime of the  $C\ 1s$ , around 0.1 eV [24,25]. ARPES data from the parent system  $C_{60}/Cu(111)$  are in line with the present results. In that case the strong hybridization at the  $C_{60}/metal$  interface significantly modifies the electronic structure of the molecular layer, causing the appearance of an extra dispersing peak within the HOMO-LUMO gap [30]. Compared to  $C_{60}$  monolayers on other noble metals, our results indicate that the interaction of  $C_{60}$  with  $Cu(553)$  is stronger than for  $Au(110)$  [24] and the vicinals  $Ag(554)$  and  $Au(443)$ , for which some intensity is still detected at the HOMO resonance. In the case of  $C_{60}/Al$ , although the chemical bond to the substrate is predominantly covalent [31], the HOMO resonance has been clearly observed in the ML system. This suggests us that the short lifetime of the excited state in  $C_{60}/Cu(553)$  is not only due to the strength of the bonding but also to the specific  $C_{60}/metal$  electronic structure.

From our experimental data, it can also be inferred that for  $C_{60}/Cu(553)$  it is not possible to localize the core-hole in a particular region of the  $C_{60}$  molecule by selecting the direction of the electric vector. Some degree of localization for electrons excited to the LUMO in C atoms from the sides of the molecule, which are not in contact with the substrate, could have been expected. As a test, we also performed resonant photoemission with the electric vector perpendicular to the surface, which should locate a hole on the top part of the molecule (data not shown). However in all cases we found no traces of HOMO resonance, meaning that the hybridization with the substrate affects the whole  $C_{60}$  molecule, in contrast with results on  $C_{60}/Al(111)$  and  $Al(110)$  [25]. On the other hand, the second  $C_{60}$  layer is much less affected by hybridization to the substrate, as demonstrated by the presence of the HOMO participator and spectator features in the curve (a) of Fig. 4.

## 5. Summary

In conclusion, our resonant photoemission study of  $C_{60}$  monolayers on  $Cu(553)$  shows that the excited electron delocalizes on a time-scale faster than the  $C\ 1s$  lifetime, probably due to hybridization of the LUMO orbital with the substrate. Consistently, NEXAFS and XPS data show signs of strong molecule-substrate interaction. The core-hole weight appears to be distributed in all the molecule and isotropic charge transfer to the substrate is observed.

## Acknowledgement

Technical support from C. Hess and F. Dubi is gratefully acknowledged.

## References

- [1] R.F. Service, *Science* 295 (5564) (2002) 2398.
- [2] G.M. Whitesides, J.P. Mathias, C.T. Seto, *Science* 254 (5036) (1991) 1312.
- [3] F.J. Himpsel, J.L. McChesney, J.N. Crain, A. Kirakosian, V. Perez-Dieste, N.L. Abbott, Y.Y. Luk, P.F. Nealey, D.Y. Petrovykh, *J. Phys. Chem. B* 108 (2004) 14484.
- [4] K. Kuhnke, K. Kern, *J. Phys. Condens. Mat.* 15 (2003) S3311.
- [5] R.R. Fasel, A. Cossy, K.H. Ernst, F. Baumberger, T. Greber, J. Osterwalder, *J. Chem. Phys.* 115 (2001) 1020.
- [6] L. Gavioli, M. Finetti, M. Sancrotti, M. Betti, *Phys. Rev. B* 72 (2005) 035458.
- [7] F. Schiller, M. Ruiz-Oses, J.E. Ortega, P. Segovia, J. Martinez-Blanco, B.P. Doyle, V. Perez-Dieste, J. Lobo, N. Neel, R. Berndt, J. Kroger, *J. Chem. Phys.* 125 (2006) 144719.
- [8] A. Tamai, W. Auwärter, C. Cepek, F. Baumberger, T. Greber, J. Osterwalder, *Surf. Sci.* 566–568 (2004) 633.
- [9] N. Neel, J. Kroger, R. Berndt, *Appl. Phys. Lett.* 88 (16) (2006) 163101.
- [10] A. Tamai, A.P. Seitsonen, T. Greber, J. Osterwalder, *Phys. Rev. B* 74 (2006) 085407.
- [11] H. Park, J. Park, A.K. Lim, E. Anderson, P. Alivisatos, P. McEuen, *Nature* 407 (2000) 57.
- [12] O. Gunnarsson, *Alkali-doped fullerenes: narrow-band solids with unusual properties*, World Scientific Publishing Co. Pte. Ltd., Singapore, 2004.
- [13] K.-D. Tsuei, P. Johnson, *Solid State Commun.* 101 (1997) 337.
- [14] C.-T. Tzeng, W.-S. Lo, J.-Y. Yuh, R.-Y. Chu, K.-D. Tsuei, *Phys. Rev. B* 61 (2000) 2263.
- [15] G.K. Wertheim, D.N.E. Buchanan, *Phys. Rev. B* 50 (15) (1994) 11070.
- [16] C. Cepek, I. Vobornik, A. Goldoni, E. Magnano, G. Selvaggi, J. Kroger, G. Panaccione, G. Rossi, M. Sancrotti, *Phys. Rev. Lett.* 86 (14) (2001) 3100.
- [17] J. Schlappa, C. Schussler-Langeheine, R. Scherer, L. Tjeng, *Phys. Rev. Lett.* 93 (2004) 119701.
- [18] C. Cepek, I. Vobornik, A. Goldoni, E. Magnano, G. Selvaggi, J. Kroger, G. Panaccione, G. Rossi, M. Sancrotti, *Phys. Rev. Lett.* 93 (2004) 119702.
- [19] W.L. Yang, V. Brouet, X.J. Zhou, H.J. Choi, S.G. Louie, M.L. Cohen, S.A. Keller, P.V. Bogdanov, A. Lanzara, A. Goldoni, F. Parmigiani, Z. Hussain, Z.X. Shen, *Science* 300 (5617) (2003) 303.
- [20] A. Tamai, Ph.D. dissertation, Universität Zürich.
- [21] P.A. Brühwiler, O. Karis, N. Märtensson, *Rev. Mod. Phys.* 74 (2002) 703.
- [22] J. Schnadt, P.A. Brühwiler, L. Patthey, J.N. O'Shea, S. Sodergren, M. Odelius, R. Ahuja, O. Karis, M. Bassler, P. Persson, H. Siegbahn, S. Lunell, N. Märtensson, *Nature* 418 (2002) 620.
- [23] A. Fohlich, P. Feulner, F. Hennies, A. Fink, D. Menzel, D. Sanchez-Portal, P.M. Echenique, W. Wurth, *Nature* 436 (2005) 373.
- [24] A.J. Maxwell, P.A. Brühwiler, A. Nilsson, N. Märtensson, P. Rudolf, *Phys. Rev. B* 49 (1994) 10717.
- [25] A.J. Maxwell, P.A. Brühwiler, D. Arvanitis, J. Hasselström, N. Märtensson, *Phys. Rev. Lett.* 79 (8) (1997) 1567.
- [26] K.D. Tsuei, J.Y. Yuh, C.T. Tzeng, R.Y. Chu, S.C. Chung, K.L. Tsang, *Phys. Rev. B* 56 (23) (1997) 15412.
- [27] T.R. Ohno, Y. Chen, S.E. Harvey, G.H. Kroll, J.H. Weaver, R.E. Haufler, R.E. Smalley, *Phys. Rev. B* 44 (24) (1991) 13747.
- [28] A. Nilsson, O. Bjorneholm, E.O.F. Zdansky, H. Tillborg, N. H Märtensson, J.N. Andersen, R. Nyholm, *Chem. Phys. Lett.* 197 (1–2) (1992) 12.
- [29] P.A. Brühwiler, A.J. Maxwell, P. Rudolf, C.D. Gutleben, B. Wastberg, N. Märtensson, *Phys. Rev. Lett.* 71 (1993) 3721.
- [30] A. Tamai, A. Seitsonen, F. Baumberger, M. Hengsberger, Z.-X. Shen, T. Greber, J. Osterwalder, *Phys. Rev. B* 77 (2008) 075134.
- [31] A.J. Maxwell, P.A. Brühwiler, D. Arvanitis, J. Hasselström, M.K.J. Johansson, N. Märtensson, *Phys. Rev. B* 57 (12) (1998) 7312.